

## References and Notes

- (1) Singler, R. E.; Hagnauer, G. L. *Polyphosphazenes: Structure and Applications*; Academic Press: New York, 1978.
- (2) Allcock, H. R.; Fuller, T. J.; Matsumura, K.; Austin, P. E. *Polym. Prepr. (Am. Chem. Soc., Div. Polym. Chem.)* **1983**, *21*, 111.
- (3) Kojima, M.; Magill, J. H. *Polymer* **1985**, *26*, 1971.
- (4) Alexander, M. N.; Desper, C. R. *Macromolecules* **1977**, *10*, 721.
- (5) Sun, D. C.; Magill, J. H. *Polym. Pap.* **1987**, *28*, 1243.
- (6) Kojima, M.; Magill, J. H. *Polymer* **1989**, *30*, 579.
- (7) Price, F. P.; Wendorf, J. H. *J. Phys. Chem.* **1971**, *75*, 2839.
- (8) Price, F. P.; Wendorf, J. H. *J. Phys. Chem.* **1971**, *75*, 2849.
- (9) Price, F. P.; Wendorf, J. H. *J. Phys. Chem.* **1972**, *76*, 276.
- (10) Price, F. P.; Fritzsche, J. *J. Phys. Chem.* **1973**, *77*, 386.
- (11) Jabarin, S. A.; Stein, R. S. *J. Phys. Chem.* **1973**, *77*, 399.
- (12) Jabarin, S. A.; Stein, R. S. *J. Phys. Chem.* **1973**, *77*, 409.
- (13) Adamski, P.; Czyzewski, R. *Sov. Phys. Crystallogr.* **1978**, *23*, 82.
- (14) Adamski, P.; Czyzewski, R. *Sov. Phys. Crystallogr.* **1977**, *22*, 725.
- (15) Warner, S. B.; Jaffe, M. *J. Cryst. Growth* **1980**, *48*, 184.
- (16) Grebowicz, J.; Cheng, S. Z. D.; Wunderlich, B. *J. Polym. Sci., Polym. Phys. Ed.* **1986**, *24*, 675.
- (17) Liu, X.; Hu, S.; Xu, M.; Zhou, Q.; Duan, X. *Polymer* **1989**, *30*, 273.
- (18) Masuko, T.; Okuizumi, K.; Yonetake, K.; Magill, J. H. *Macromolecules* **1989**, *22*, 4636.
- (19) Mujumdar, A.; Young, S. G.; Merker, R. L.; Magill, J. H. *Makromol. Chem.* **1990**, *190*, 2293.
- (20) Magill, J. H. *Nature* **1960**, *187*, 770-771.
- (21) Turnbull, D.; Fisher, J. C. *J. Chem. Phys.* **1949**, *17*, 71-74.
- (22) Wunderlich, B. *Macromolecular Physics*; Academic Press: New York, 1976; Vol. 2.
- (23) Magill, J. H. In *Treatise on Materials Science and Technology*; Academic Press: New York, 1977; Vol. 10A.
- (24) Hoffman, J. D.; Davis, G. T.; Lauritzen, J. I., Jr. *Treatise on Solid State Chemistry*; Plenum Press: New York, 1972.
- (25) Young, S. G.; Magill, J. H. *Macromolecules* **1989**, *22*, 2549.

Registry No. PBFP, 28212-50-2.

## A Study of the Isothermal Crystallization Kinetics of Polyphosphazene Polymers. 3. Poly[bis(phenylphenoxy)phosphazene]

Richard J. Ciora, Jr., and Joseph H. Magill\*

*Material Science and Engineering Department, University of Pittsburgh, Pittsburgh, Pennsylvania 15261. Received July 24, 1989;  
Revised Manuscript Received November 7, 1989*

**ABSTRACT:** In this study the isothermal crystallization kinetics of poly[bis(phenylphenoxy)phosphazene] have been examined utilizing (i) a modified differential scanning calorimeter (DSC) technique and (ii) a depolarized light intensity (DLI) technique. The kinetics of transformation of the isotropic to 2-D pseudo-hexagonal mesophase (i.e. the sub  $T_m$  transformation) as well as the mesophase to 3-D orthorhombic phase (i.e. the sub  $T(1)$  transformation) have been measured and analyzed by using Avrami analysis. Classical nucleation theory has been applied for estimating the surface free energy values for nucleation/crystallization behavior corresponding to the phase transformations in the sub  $T(1)$  and sub  $T_m$  regions. These results have been compared with poly[bis(trifluoroethoxy)phosphazene]. It has been found that the polymers display similar transformation kinetics. Both show very high, negative growth rates versus inverse undercooling coefficients as well as inordinately small surface free energy products compared to normal homopolymers, in accord with the compatibility of the mesophase transformation interfaces.

## Introduction

Since the 1960s many stable linear high molecular weight polyphosphazene polymers have been synthesized, and some of their physical and thermal properties have been characterized. The basic structure of these polymers consists of an alternating phosphorous and nitrogen backbone as shown in Figure 1. Because of the variety of substituent groups that may be attached to the phosphorous atom, an extensive array of polymers with diverse properties can be produced.<sup>1,2</sup>

Many of the semicrystalline polyphosphazenes exhibit three thermal transitions on heating; a glass transition at  $T_g$ , a mesomorphic transition at  $T(1)$  from the three dimensionally ordered orthorhombic ( $\gamma$ -form) crystalline state to the two dimensionally ordered pseudo-hexagonal ( $\delta$ -form) state followed by isotropization at  $T_m$ . Recently, considerable interest has focused on determining the structure of these polymers in both the crystalline and mesomorphic states as it relates to the sample's thermal history.<sup>3,4</sup> Although considerable effort has gone

into elucidating the structure of these materials in the various phases, few investigations into molecular aspects of the mechanisms and energetics that control the formation of these phases in polyphosphazenes have been conducted.<sup>5-7</sup> A basic understanding of the energetics and mechanisms of the formation of the different phases and their dependence on thermal history is necessary from a physical properties perspective because such properties as toughness, elasticity, permeability, etc. can be significantly altered by polymeric microstructure. It is through isothermal bulk crystallization studies that such information may be obtained.

In this paper the kinetics of the isothermal crystallization of the polyphosphazene polymer poly[bis(phenylphenoxy)phosphazene] or PB(4-Ph)PP (shown in Figure 1) are investigated by using the depolarized light intensity<sup>8</sup> (DLI) technique. In part I<sup>9</sup> of this series the DLI technique had been examined as a general technique for studying phase transformations in polyphosphazene polymers. In part II kinetic measurements<sup>5</sup> for the crystallization transformation in poly[bis(trifluoro-

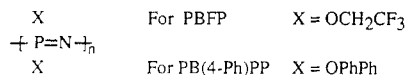


**Figure 1.** The basic alternating phosphorous-nitrogen structure of the poly(phosphazene) polymer.

**Table I**  
**Characterization Data of the PB(4-Ph)PP Sample**

	PB(4-Ph)PP
density ( $\gamma$ -form) <sup>a</sup>	1.3 g/cm <sup>3</sup>
unit cell dimens (orthorhombic)	
$a_0$	4.18 nm <sup>11</sup>
$b_0$	1.83 nm <sup>11</sup>
$c_0$	0.96 nm <sup>11</sup>
unit cell dimens (hexagonal form) <sup>b</sup>	
$a(220^\circ\text{C})$	1.81 nm
mesophase transition temp, $T(1)$	218.2 °C
melting transition temp, $T_m$	280.3 °C
glass transition temp, $T_g$	85 °C
$\Delta H_f$ at $T_m$	6.28 J/g
$\Delta H_f$ at $T(1)$	89.2 J/g

<sup>a</sup>  $\gamma$ -form designates the 3-D orthorhombic structure of many of the poly(phosphazene) polymers. <sup>b</sup> Hexagonal form designates the general structure of the 2-D mesophase of these polymers.

ethoxy)phosphazene] or PBFP (also shown in Figure 1) were conducted by using both a modified differential scanning calorimetry technique as well as the DLI technique. The results from both techniques are in agreement, but the DLI technique was found to be a superior method for investigating specific crystallization transformations. Two major factors are responsible, namely: (1) the DLI technique could be utilized to study a wider range of supercoolings because of the rapid rate of response of the photodiode light detector to rapid changes in sample birefringence and (2) it was more sensitive to small changes in the crystallization transformations since the overall transformation process was being measured, not its derivative as measured by the DSC. For these reasons no kinetic measurements are reported using the DSC technique.

The objectives of this research mimic those of the previous paper: (1) to establish and quantify the rate at which PB(4-Ph)PP crystallizes, (2) to establish the type and/or mode of crystallization by which this polymer crystallizes, and (3) to examine the nature and energetics of the crystallization process in this polymer. A secondary objective of this paper is to examine the similarities and differences in the crystallization behavior of the two polymers, specifically PB(4-Ph)PP, a phenoxy-substituted polyphosphazene, and PBFP, an alkyl-substituted polyphosphazene.

## Experimental Section

**Material and Equipment.** In this study poly[bis(phenylphenoxy)phosphazene], PB(4-Ph)PP, was synthesized via the solution polymerization technique<sup>10</sup> and was characterized by DSC, X-ray, and <sup>31</sup>P solution NMR. The NMR results indicated that the polymer was linear. The DSC and X-ray characterization data are provided in Table I.

DLI measurements were conducted by using the instrumental equipment described in part 2. Isothermal crystallization measurements were carried out in the sub  $T_m$  and sub  $T(1)$  regions for PB(4-Ph)PP. The experimental runs were conducted by using the following procedures. In the sub  $T_m$  region (isotropic melt to 2-D mesophase transformation), the sample was first fused at 290 °C ( $T_m + 8^\circ\text{C}$ ) for 10 min to remove previous thermal history and then quenched to the desired crystallization temperature at roughly 25 °C/min. For experimental measurements in the sub  $T(1)$  region (2-D mesophase to 3-D crystalline transformation), a sample was again fused at 290

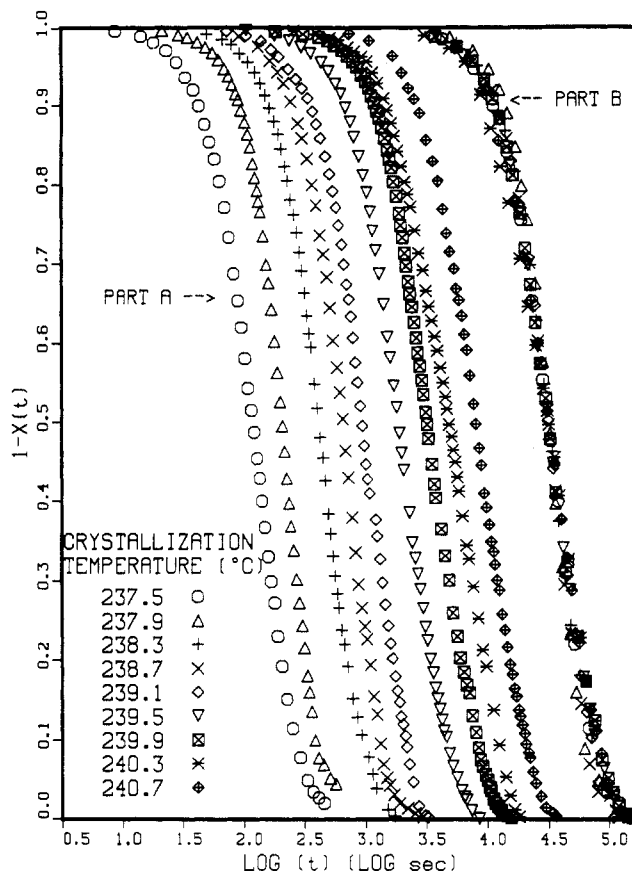


**Figure 2.** The extent of transformation versus log time curves for PB(4-Ph)PP at several crystallization temperatures for the isotropic melt to 2-D mesophase transformation. Part A: the actual curves. Part B: these curves when superimposed.

°C for 10 min, then quenched to 230 °C, and crystallized for 30 min to freeze in the 2-D mesophase. Afterwards the sample was quenched to the desired crystallization temperature in the sub  $T(1)$  region. DLI measurements were made when thermal equilibrium was reached. Without the two-step procedure, the end of the isotropic to 2-D transformation would be superimposed onto the 2-D to 3-D transformation.

To elucidate morphological details during phase transformations, photomicrographs were taken in both the sub  $T_m$  and sub  $T(1)$  regions for PB(4-Ph)PP with a Leica 35-mm camera using Kodak Tri-X pan (ASA 400) film.

## Theory

The mode of nucleation and subsequent crystallite growth and the overall rate of crystallization in these polymers have been successfully characterized utilizing the familiar Avrami analysis. The energetics associated with the formation of nuclei during crystallization have been characterized via classical nucleation theory. Details pertinent to these theories have been presented in part 2 and will not be discussed here.

## Results and Discussion

**Transformations in PB(4-Ph)PP. (a) Isotropic Melt to 2-D Region.** Curves of the extent of conversion versus log time for the isotropic melt to two dimensional pseudo-hexagonal mesophase transformation in PB(4-Ph)PP are shown in Figure 2. The good superposability of these curves, as illustrated in part B of this figure, indicates the mechanism controlling the crystallization in this polymer is invariant over the range of temperatures shown. From this data it is possible to generate the Avrami plots which are shown in Figure 3. From the slope of the initial linear portion of these curves the Avrami

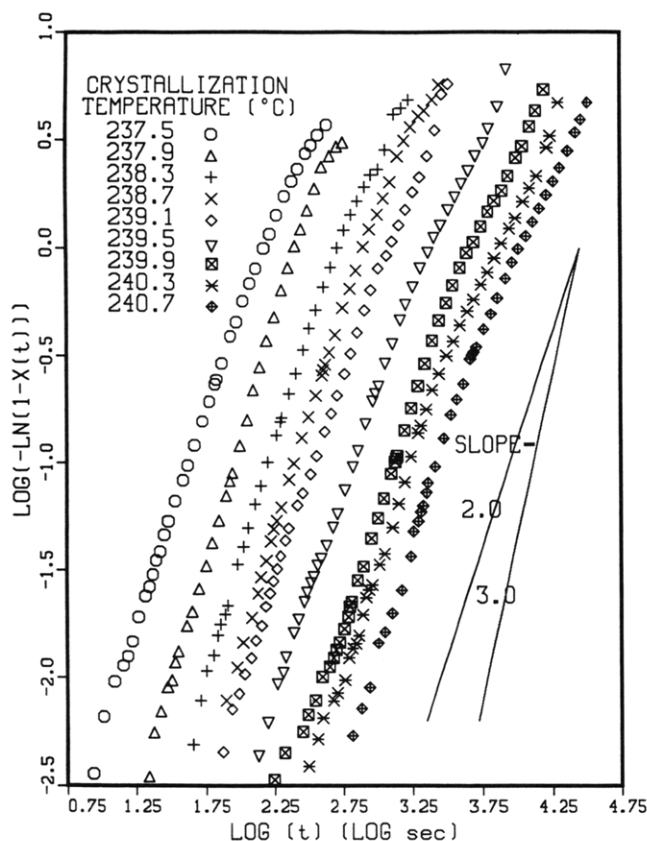


**Figure 3.** Avrami plots for the isotropic melt to 2-D mesophase transformation in PB(4-Ph)PP.

**Table II**  
Values for the Avrami Parameters,  $n$  and  $k$ , for the Isotropic Melt to 2-D Mesophase Transformation in PB(4-Ph)PP Obtained from the DLI Measurements

$T_c$ , °C	$\Delta T$ , °C	$n$	$10^7 k$ , s $^{-2.0}$
237.5	42.5	1.96	49300
237.9	42.1	2.22	16600
238.3	41.7	2.14	4080
238.7	41.3	2.15	1630
239.1	39.9	1.95	776
239.5	39.5	1.93	199
239.9	39.1	1.91	53.0
240.3	38.7	1.87	27.6
240.7	38.3	2.06	10.7

$$n_{av} = 2.02 \pm 0.12$$

nucleation and growth parameter,  $n$ , may be obtained. Linear least-squares analysis yielded an average  $n$  of  $2.02 \pm 0.12$  over the crystallization range examined. The Avrami  $k$  parameters were determined at a fractional conversion of 0.3 by using an approximate  $n$  of 2. The individual values for  $n$  and  $k$  for the plots of Figure 3 are listed in Table II.

Shown in Figures 4 and 5 are photomicrographs of this transformation at several different times for the crystallization temperatures of 239.5 and 238.7 °C. When the micrographs at constant  $T_c$  and at different times are compared, it can be concluded that the nucleation is athermal, since no new nuclei appear over the entire time of crystallization after initial nucleation. Because of the proximity to the melting temperature, it may also be concluded that the nucleation is probably heterogeneous in nature. Since the primary nucleation proves to be athermal and heterogeneous and the Avrami nucleation parameter is approximately 2, it may be concluded that the growth habit of the crystallites is two-dimensional or plate-like from heterogeneous, athermally formed nuclei.

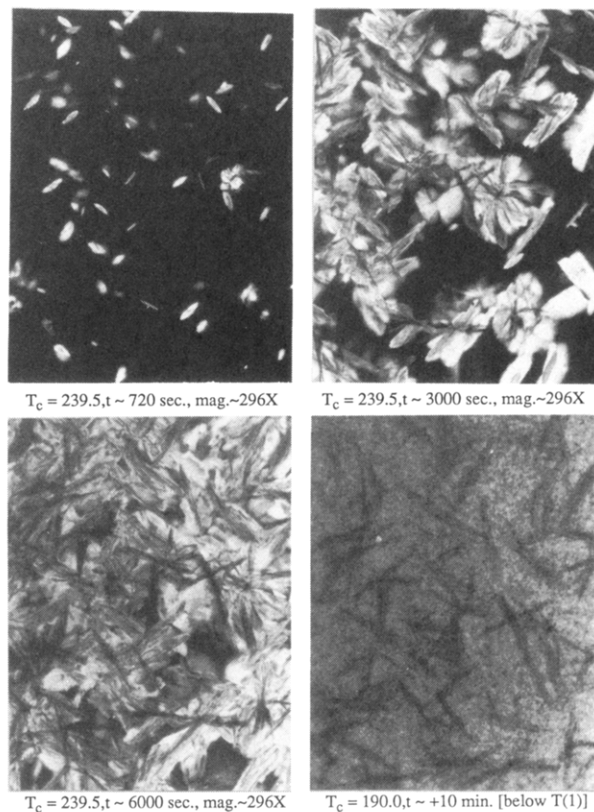


**Figure 4.** Photomicrographs (a) through (c) show the isotropic melt to 2-D mesophase transformation in PB(4-Ph)PP and (d) shows the resultant texture when quenched below  $T(1)$  (i.e. the 2-D to 3-D transformation).

Plots of  $\ln k$  versus  $1/T_c \Delta T$  and  $1/T_c \Delta T^2$  for this transformation are shown in Figure 6. It is apparent from these curves and Table II that the rate constants for this transformation vary significantly over a small range of undercooling, increasing substantially as the driving force for crystallization increases. This is indicative of nucleation control of the transformation through the primary and/or secondary nucleation steps. Since the plot of  $\ln k$  versus  $1/T_c \Delta T$  yields the best straight line fit to the data, with slope  $-253\,000\text{ K}^2$ , it will be used to examine the energetics involved in this transformation. As was shown in part 2 for PBFP, if 2-D heterogeneous primary nucleation is applicable to this transformation, then from the slope of this plot the product of the surface energies associated with the formation of the secondary nuclei may be calculated through an equation of the form

$$\text{slope} = -4zb_0\sigma\sigma_e T_m^0 / k_b \Delta H \quad (1)$$

For PB(4-Ph)PP,  $b_0 = 1.81\text{ nm}$ ,  $\Delta H = 8.162\text{ J/cm}^3$ , and  $z = 2$ , since the crystallite growth dimensionality was 2 from the results of the Avrami analysis. Hence the product of the surface energies,  $\sigma\sigma_e$ , is  $5.0\text{ ergs}^2/\text{cm}^4$ . This value is several orders of magnitude less than surface free energy products found for normal homopolymers<sup>12</sup> (polyethylene  $\sim 1280$ , i-polystyrene  $\sim 266$ , poly(chlorotrifluoroethylene)  $\sim 200\text{ ergs}^2/\text{cm}^4$ , and poly(TMPS)<sup>13,14</sup>  $\sim 70\text{--}140\text{ ergs}^2/\text{cm}^4$  depending upon molecular weight) that crystallize directly from the isotropic melt to the three-dimensional crystalline phase. It is comparable, however, to the value obtained for the same transformation in PBFP which was found to be  $1.6\text{ ergs}^2/\text{cm}^4$ .

**(b) 2-D to 3-D Region.** The transformations from the two-dimensional (pseudohexagonal) mesophase to three-dimensional orthorhombic phase as a function of log time are shown in Figure 7. As in the higher temperature trans-

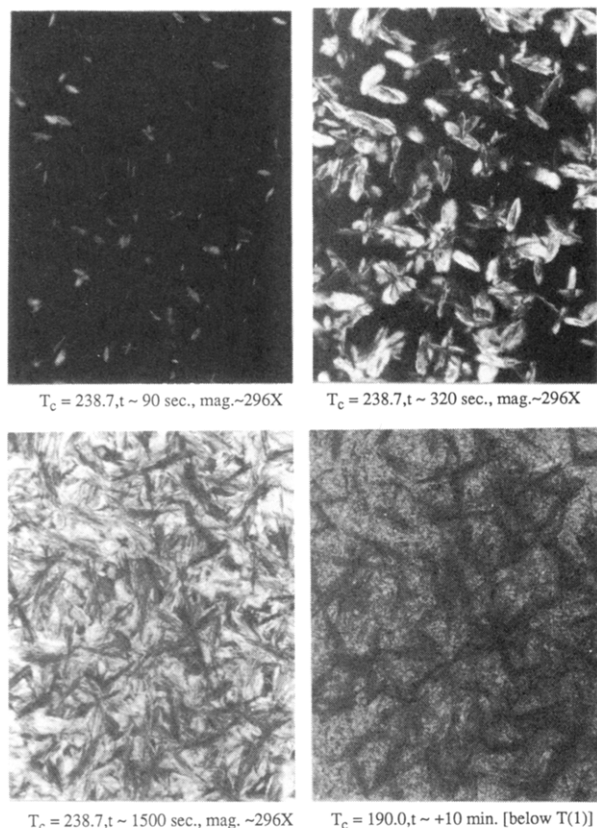


**Figure 5.** Photomicrographs (a) through (c) show the isotropic melt to 2-D mesophase transformation in PB(4-Ph)PP and (d) shows the resultant texture when quenched below  $T(1)$  (i.e. the 2-D to 3-D transformation).

formations, these curves show good low conversion superposability, this being evidence for a nucleation and growth mechanism that is constant over the crystallization temperature range studied. Avrami plots of this data are shown in Figure 8.

Avrami  $n$  and  $k$  data generated from these plots are given in Table III. The individual nucleation parameters,  $n$ 's, were evaluated by a least-squares fit of the data in the initial linear portion of each curve. An average value of  $n$  was determined to be  $2.08 \pm 0.12$ . The rate parameters were evaluated at a fractional conversion of 0.25 based on an estimated value of  $n$  of 2. Photomicrographs of this transformation are shown in Figures 4 and 5. These micrographs illustrate that the transmitted light intensity through the sample decreases as the transformation from the 2-D to 3-D state proceeds. However, since parts c to d of Figure 4 and parts c to d of Figure 5 offer no clear optical indication as to the mode of nucleation, it is not possible to conclusively establish the growth habit of the crystallites from the Avrami  $n$ . Therefore another method must be utilized to determine the mode of nucleation.

From Table III it is evident that (i) the rate constants increase markedly with small increases in supercooling and that (ii) relatively small values of supercooling (about 18 °C) are necessary to induce crystallization in these samples. The small supercooling is indicative of heterogeneous nucleation of the sample. On the basis of this evidence, it appears that, given an Avrami  $n$  of 2, the growth of the crystallites is two-dimensional and plate-like from athermal, heterogeneous nuclei.

Plots of  $\ln k$  versus  $1/T_c \Delta T$  and  $1/T_c \Delta T^2$ , where  $\Delta T = T(1) - T_c$ , are shown in Figure 9. From the low supercooling end of the plot versus  $1/T_c \Delta T$ , a slope of  $-189\,000\text{ K}^2$  was determined. With this value the product of the

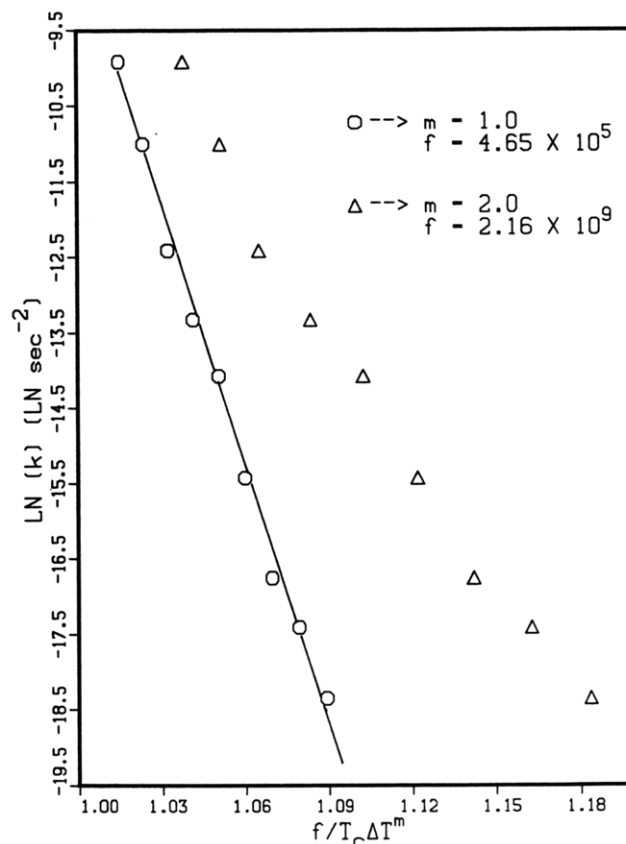


**Figure 6.** Plots of  $\ln k$  versus  $1/T_c \Delta T$  and  $1/T_c \Delta T^2$  for the isotropic melt to 2-D mesophase transformation of PB(4-Ph)PP.

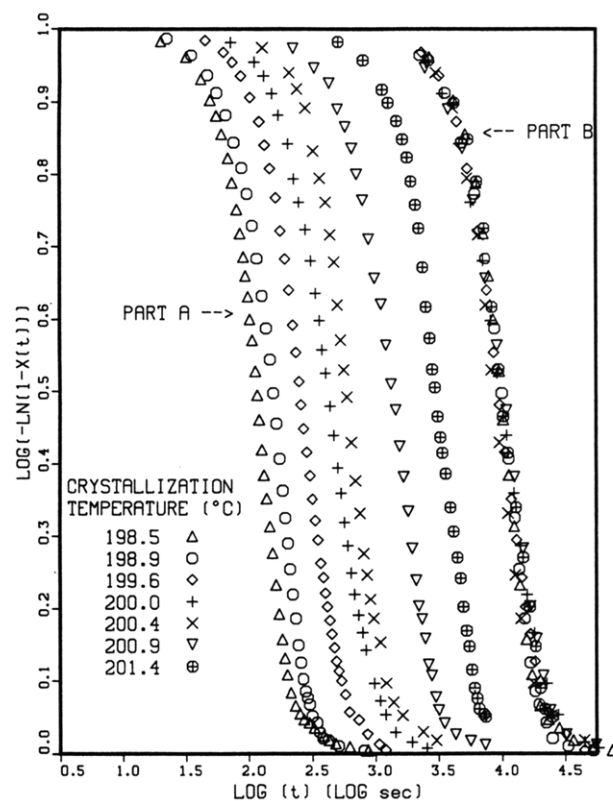


**Figure 7.** The extent of transformation versus log time curves for PB(4-Ph)PP at several crystallization temperatures for the 2-D mesophase to 3-D crystalline transformation. Part A: the actual curves. Part B: the actual curves when superimposed.

surface free energies,  $\sigma\sigma_e$ , is  $42\text{ ergs}^2/\text{cm}^4$  from eq 1 for PB(4-Ph)PP with  $b_0 = 1.83\text{ nm}$ ,  $\Delta H = 116\text{ J/cm}^3$ , and  $z$

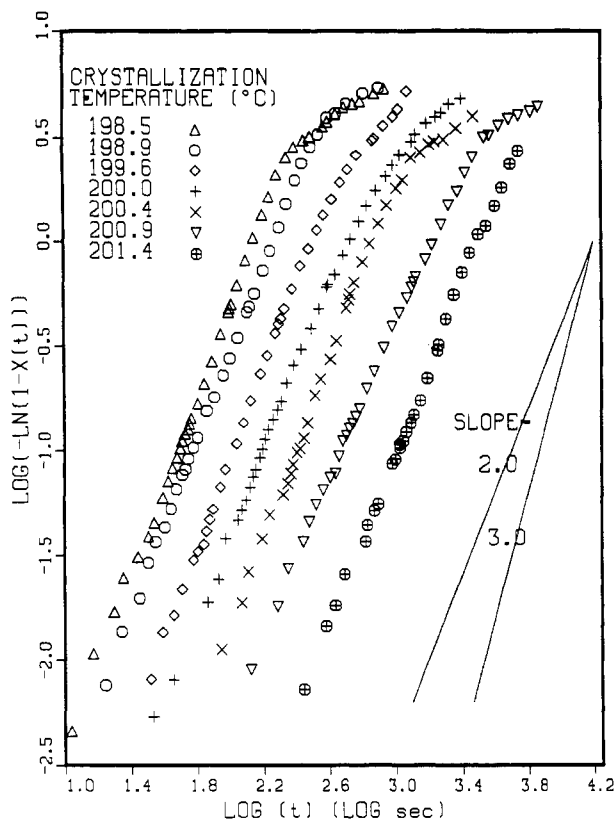


Figure 8. Avrami plots for the 2-D mesophase to 3-D crystalline transformation in PB(4-Ph)PP.

Table III  
Values for the Avrami Parameters,  $n$  and  $k$ , for the 2-D Mesophase to 3-D Crystalline Transformation in PB(4-Ph)PP Obtained from the DLI Measurements

$T_c$ , °C	$\Delta T$ , °C	$n$	$10^7 k$ , s $^{-2.0}$
198.5	19.5	2.16	48000
198.9	19.1	2.03	29200
199.6	18.4	2.18	10700
200.0	18.0	2.07	5210
200.4	17.6	2.23	1750
200.9	17.1	1.86	450
201.4	16.6	2.10	71.1

$$n_{av} = 2.09 \pm 0.12$$

= 2. For a similar transformation in PBFP (in part 2),  $\sigma\sigma_e$  was found to be 30 ergs $^2$ /cm $^4$ . Thus the two polymers display comparable surface free energy products. These values are at least an order of magnitude less than are obtained for melt to crystalline transformations in normal homopolymers.

Finally, it is puzzling that the  $\sigma\sigma_e$  interfacial energy products determined here for the (i) isotropic to 2-D and (ii) 2-D to 3-D transformations exhibit low values for these PBFP and PB(4-Ph)PP polymers considering that the molecules of the crystallites are in the chain-extended conformation. This fact is contrary to the classical interpretation $^{12}$  that surface roughening (chain ends or other topological features other than regular folds) leads to high  $\sigma_e$  values. However, a plausible explanation for the lower surface free energy values appears to reside in the side-chain mobility conferred through the oxygen linkage which enhances the interphase compatibility in the sub  $T_m$  and sub  $T(1)$  regions.

## Conclusions

The mechanisms for the nucleation and growth of these two polyphosphazene polymers, PB(4-Ph)PP and PBFP,

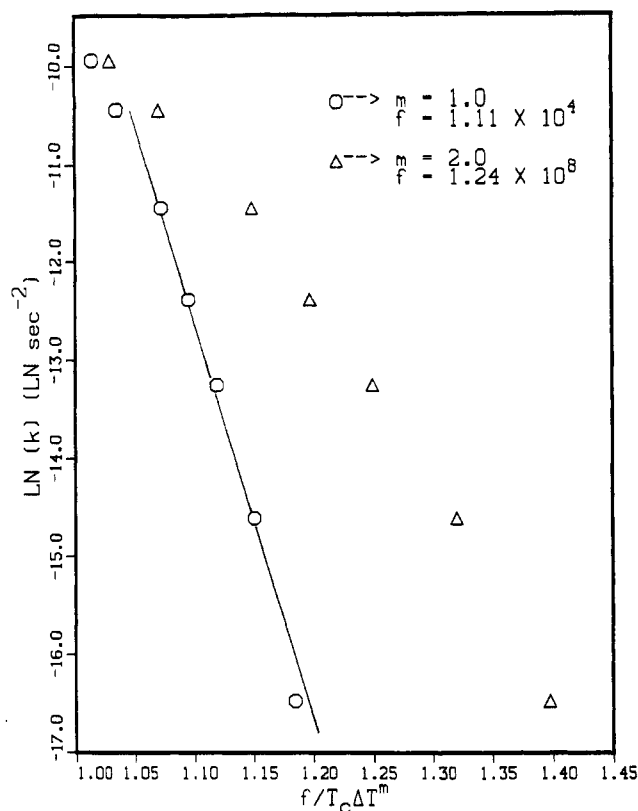


Figure 9. Plots of  $\ln k$  versus  $1/T_c \Delta T$  and  $1/T_c \Delta T^2$  for the 2-D mesophase to 3-D crystalline transformation in PB(4-Ph)PP.

have been established here for both the isotropic to 2-D mesophase as well as the 2-D mesophase to 3-D crystal transformations. Several conclusions concerning these transformations are enumerated below.

For the isotropic melt to 2-D mesophase transformation, the following has been established:

(1) From the analysis of the crystallization kinetics, it was found that both polymers displayed similar mechanisms of nucleation and growth for this transformation. The transformation in each case was consistent with athermal, heterogeneous nucleation followed by macroscopic growth in only two dimensions resembling platelike growth.

(2) The degree of supercooling necessary to induce crystallization in these polymers was significantly different. PB(4-Ph)PP was found to require a much larger supercooling to initiate crystallization compared to PBFP, indicating the formation of PB(4-Ph)PP crystallites required the greater driving force.

(3) The products of the side surface and end surface free energies,  $\sigma\sigma_e$ , of the secondary nuclei were found to be 1.6 and 5.0 ergs $^2$ /cm $^4$  for PBFP and PB(4-Ph)PP, respectively. Although these are estimated values, they are small compared to normal homopolymers. In conjunction with the low enthalpies of transition, they indicate that small forces hold the mesophases together.

(4) The side groups seem to play an important role only in the energetics of the formation of the nuclei, the larger the side group (PB(4-Ph)PP) the larger the supercooling and surface free energies associated with the phase transformation. It is apparent however that the group size has no effect on (i) the dimensionality of the nuclei and of the crystallites or (ii) the nucleation parameter,  $n$ .

For the 2-D mesophase to 3-D ordered crystal transformation, the conclusions are as follows:

(1) The mechanism for this transformation appears similar for PB(4-Ph)PP and PBFP, yielding from kinetic

experiments a nucleation parameter of two. Since photomicrographs revealed little about this transformation in PB(4-Ph)PP (and nothing useful for PBFP because of the small light intensity change through this transition), it was difficult to determine the mode of nucleation. However, it can be expected that due to the low undercoolings necessary for these transformations and the large and negative temperature dependence of rate constants, heterogeneous, athermal nucleation should prevail. Thus coupled with an Avrami  $n$  of 2, the growth habit must be two-dimensional in nature.

(2) The product of the surface free energies associated with the formation of the secondary nuclei were estimated to be 30 and 42 ergs<sup>2</sup>/cm<sup>4</sup> for PBFP and PB(4-Ph)PP, respectively, for this transformation. Again, the energies are small, by at least an order of magnitude, compared to several normal homopolymers that do not exhibit mesophase transitions. It is interesting that the low  $\sigma_e$  evaluated classically for the isotropic to 2-D pseudo-hexagonal and 2-D to 3-D orthorhombic transformations in these two polymers (which form chain-extended molecules) is contrary to the notion that surface roughening<sup>12</sup> (associated with chain ends, for example) leads to high  $\sigma_e$  values.

(3) The larger degree of supercooling and the slower rate of crystallization of PB(4-Ph)PP over PBFP suggest that the bulkier phenylphenoxy side group is more difficult to crystallize. Therefore the side group chemistry and size as in the isotropic to two-dimensional transformation affect the extent of undercooling and rate of crystallization but do not affect the mechanism by which nucleation and growth occurs.

**Acknowledgment.** Thanks are due to the National Science Foundation (Polymer Program, Grant DMR 8509412) and the Office of Naval Research (Chemistry Program, Grant N0001485K0358) for research support. We also wish to thank Dr. T. Nishikawa of the Nippon Soda Co. for supplying the polymerization grade trimer used for the synthesis of these polyphosphazenes and Dr. F.-T. Lin, Chemistry Department, University of Pittsburgh, for the solution NMR analysis.

## Appendix

The DLI method for recording isothermal crystallization transformations in polymers has been used sporadically since its inception as a viable technique in the 1950's. Binsbergen,<sup>15</sup> however, pointed out a problem associated with the depolarization technique and the Avrami theory. He showed that for spherulites initiated athermally growing in an isotropic media, the Avrami nucleation parameter,  $n$ , should be 4 by the DLI method, not 3 as is found by other methods, specifically DSC, dilatometry, etc. The increase in  $n$  results from the dependence of the optical retardation ( $\delta$ ) on the square of the crystallites thickness ( $t_h^2$ ) assuming  $\delta \ll 1$ . We agree with this conclusion. However, it is questionable that the DLI method would yield an  $n$  of 3 for a 2-D spherulite (a spherulite constrained from growth parallel to the light beam by the coverslips) as is suggested by Binsbergen but would instead yield an  $n$  of 2, the standard Avrami result, since the thickness of the growing 2-D spherulite is not changing. As such the DLI results would then agree with other experimental methods for determining Avrami kinetic parameters for 2-D spherulites.

This conclusion has a significant impact on the work presented in this paper and previously in part 2, since it can be shown that for any crystallite growing in two dimensions, the DLI method would yield an  $n$  of 2, the stan-

dard Avrami result, not 3, as is suggested by Binsbergen.<sup>15</sup> Only when one of the two crystallite growth directions is *exactly* parallel to the light beam, will an  $n$  of 3 result. This situation is impossible for a 2-D spherulite considering the definition given above and is of very limited importance for 2-D platelets. Inspection of the original equations<sup>15</sup> will clarify these results.

The  $n = 2$  result for 2-D spherulites or plates can be derived from Binsbergen's work.<sup>15</sup> It is necessary to review part of his formulation of the mean depolarization,  $\Delta$  ( $=I_{\text{transmitted}}/I_{\text{incident}}$ ), of plane polarized light transmitted through a sample. Following Binsbergen's argument the entire sample is divided into a large number of piles,  $N_p$ , parallel to the incident light beam and of cross sectional area,  $A$ . As a crystallite grows within the sample, the number of piles it intersects will increase. The mean polarization for such a model was shown to be of the form

$$\Delta \sim Ft_h \quad (2)$$

(similar to eq 26 of Binsbergen's paper<sup>15</sup>) for uniaxially birefringent crystallites growing in an isotropic, nonbirefringent matrix, where  $F$  is the average number of crystallites per pile and  $t_h$  is the thickness of the crystallites.  $F$  may be calculated from the volume fraction of crystalline material through the simple formula<sup>16</sup>

$$V_c = \frac{N_p F t_h A}{N_p D A} \quad (3)$$

where  $D$  is the overall sample thickness ( $N_p F t_h A$  is the crystalline volume and  $N_p D A$  is the sample volume). This equation is similar to Binsbergen's<sup>15</sup> eq 27. For a 3-D crystallite (spherulite) nucleated athermally and growing at a linear growth rate,  $v$ ,  $t_h$  becomes  $vt$  ( $t$  is time) or more compactly,  $w$ , and the crystalline volume fraction is simply

$$V_c = Nw^3 \sim w^3 \quad (4)$$

where  $N$  is the number of nuclei. Furthermore, the time dependence of the crystallite thickness, parallel to the light beam, is simply

$$t_h = w (=fn(t)) \quad (5)$$

and from eq 3 and 4

$$F \sim w^2 \quad (6)$$

Finally, the mean depolarization is

$$\Delta \sim (w^2)(w)^2 \sim w^4 \sim t^4 \quad (7)$$

yielding a nucleation parameter,  $n$ , of 4, i.e. the Binsbergen result. From this result the conclusion is drawn that in general the DLI method should exhibit enhanced  $n$  values by one integer over values obtained from other methods. However, another analysis is presented here to show that this generalized result to other dimensional systems is invalid.

Now consider two-dimensional spherulites activated athermally and growing at constant rates such that the crystalline volume fraction is

$$V_c \sim w^2 \quad (8)$$

and the thickness

$$t_h \sim \text{constant (not a function of time)} \quad (9)$$

since the spherulites are constrained by the coverslips. Thus for this case eq 3 yields

$$F \sim w^3/t_h \quad (10)$$



From this the average depolarization takes the form

$$\Delta \sim (w^2/t_h)(t_h) \sim w^2 t_h \sim t_h^2 \quad (11)$$

and therefore the nucleation parameter,  $n$ , is clearly 2 (not 3).

A similar analysis would be applicable to athermally activated plates growing in 2-D in almost any orientation. The only requirement is that the crystallite growth directions do not lie *exactly* parallel to the light beam. For any other orientation the thickness of any given crystallite parallel to the light beam is invariant with the time of growth so that the depolarization would be proportional to  $t^2$ . Only when one of the crystal growth directions is *exactly* parallel to the light beam (and thus the thickness of the crystallite is increasing) will the depolarization go as  $t^3$  (i.e.,  $n = n + 1$ ). Such a crystallite orientation is highly improbable if its initial placement and orientation in the sample is random. On the basis of this reasoning it follows that the number of crystallites growing parallel to the light beam is extremely small compared with those in other orientations. Consequently an average Avrami  $n$  of 2 should dominate the DLI results obtained for 2-D crystallites.

In Binsbergen's final analysis the time dependence of the thickness is not removed when making the assumption that an athermally activated 2-D spherulite (and by inference any 2-D crystallite) would result in a nucleation parameter of 3 (i.e.,  $n + 1$ ) instead of 2. We have shown that this is not the case and, by analogy, proved that in general, for 2-D crystallites with neither growth

direction oriented *exactly* parallel to the light beam, an  $n$  of 2 should be expected. Thus the results presented in our papers, parts 2 and 3, are thoroughly consistent with platelets growing in two dimensions in which neither growth direction is parallel to the light beam.

## References and Notes

- (1) Singler, R. E.; Hagnauer, G. L. *Polyphosphazenes: Structure and Applications*, Academic: New York, 1978.
- (2) Allcock, H. R.; Fuller, T. J.; Matsumura, K.; Austin, P. E. *Polym. Prepr. (Am. Chem. Soc., Div. Polym. Chem.)* **1983**, *21*, 111.
- (3) Kojima, M.; Magill, J. H. *Polymer* **1985**, *26*, 1971.
- (4) Alexander, M. N.; Desper, C. R. *Macromolecules* **1977**, *10*, 721.
- (5) Ciora, R. J., Jr.; Magill, J. H. *Macromolecules*, preceding paper in this issue.
- (6) Young, S. G.; Magill, J. H. *Macromolecules* **1989**, *22*, 2549.
- (7) Tanaka, H.; Gomez, M. A.; Tonelli, A. E.; Schilling, F. C. *Polym. Prepr. (Am. Chem. Soc., Div. Polym. Chem.)* **1988**, *29*, 440.
- (8) Magill, J. H. *Nature* **1960**, *187*, 770-771.
- (9) Masuko, T.; Okuizumi, K.; Yonetake, K.; Magill, J. H. *Macromolecules* **1989**, *22*, 4636.
- (10) Mujumdar, A.; Young, S. G.; Merker, R. L.; Magill, J. H. *Macromol. Chem.* **1990**, *190*, 2293.
- (11) Kojima, M.; Magill, J. H. *Polymer* **1989**, *30*, 579.
- (12) Hoffman, J. D.; Davis, G. T.; Lauritzen, J. I., Jr. *Treatise on Solid State Chemistry*, Plenum: New York, 1972.
- (13) Magill, J. H. *J. Appl. Phys.* **1964**, *35*, 3249.
- (14) Magill, J. H. *J. Polym. Sci., Polym. Phys. Ed.* **1967**, *5*, 89.
- (15) Binsbergen, F. L. *J. Macromol. Sci., Phys.* **1970**, *B4*, 837.
- (16) Binsbergen, F. L. Private communication.

**Registry No.** PBFP (SRU), 28212-50-2; PB(4-Ph)PP (SRU), 28212-49-9.

## The Theoretical Modulus of Biaxially Oriented Polymer Films

C. W. M. Bastiaansen,\*† P. J. R. Leblans,† and Paul Smith†

DSM Research, P.O. Box 18, 6160 MD, Geleen, The Netherlands, and Materials Department and Department of Chemical and Nuclear Engineering, University of California at Santa Barbara, Santa Barbara, California 93106. Received April 27, 1989; Revised Manuscript Received August 3, 1989

**ABSTRACT:** Young's moduli of balanced, biaxially oriented polymer films composed of single crystal elements are calculated for several hypothetical structures, in the ideal case of 100% crystallinity. The numerical data used in the computations are the mechanical properties of the single-crystal unit, in the form of the modulus or compliance tensor. Structural characteristics of equibiaxially oriented polyethylene samples indicate that the appropriate model is an aggregate of single crystals, for which the tensile modulus is calculated by Reuss-averaging the properties of the structural unit over all directions. It is predicted, in accordance with experimental observations, that the modulus of such equibiaxially oriented films is low in comparison with the axial theoretical modulus of single crystals, due to the large contribution of the shear compliance of the crystals. By contrast, calculations presented in this study indicate that structures in which a uniform distribution of strain is achieved may exhibit a very high modulus. Such materials include laminates and certain composites.

### 1. Introduction

Numerous studies have been devoted to the theoretical modulus of polymeric crystals in the direction of the macromolecular chains.<sup>1-6</sup> It has been shown that, in general, the axial crystal modulus is high (40-320 GPa) in

comparison with that of isotropic materials (1-3 GPa). These results have triggered major experimental efforts to develop routes toward uniaxially oriented materials from both flexible and rigid macromolecules.<sup>7-11</sup> Nowadays, oriented fibers and films are manufactured that exhibit extraordinarily high Young's moduli that approach the theoretical estimates.

Little attention has been paid to the theoretical limits of the stiffness of biaxially oriented structures, despite

\* DSM Research.

† University of California at Santa Barbara.